2021 43rd Annual International Conference of the
IEEE Engineering in Medicine & Biology Society (EMBC)
Oct 31 - Nov 4, 2021. Virtual Conference

Musculoskeletal Neural Network path generator for a virtual upper-limb active controlled orthosis

Alejandro Lozano, *Member, IEEE*, David Cruz-Ortiz, *Member, IEEE*, Mariana Ballesteros, Isaac Chairez

***Abstract*—In this paper, a non-parametric model of the neuromusculoskeletal system for the biceps brachii is presented. The model serves to generate angular paths for the control of a virtual active orthosis. The path generator uses a differential neural network (DNN) identifier that obtains the reference angular position and velocities using the raw electromyographic (EMG) signals as input. The model is validated using experimental data. The training and closed-loop implementation of the proposed model are described. The control strategy ensures that the user reaches a set-point with a predefined position constraint and that the device follows the natural reference path that corresponds to the raw EMG signal.**

***Index Terms*—Neuromusculoskeletal model, Differential Neural Networks, Upper-limb rehabilitation, Virtual prototype**

I. Introduction

Over the last decades, the mechanics of the neuromusculoskeletal human system have been characterized extensively to correlate muscle activity with various dynamical and kinematic behaviors [1]. Previous works have studied the implementation of mathematical mappings, from which it is important to highlight Hill-based models to obtain angular positions of a given muscle of interest. However, the vast number of unknown parameters that must be tuned in a non-adaptive manner and patient variability makes the implementation for a given individual an arduous task [2].

Artificial neural networks (ANNs) have shown an outstanding ability to approximate any continuous nonlinear functions locally. With this in mind, we establish the implementation of a differential neural network (DNN) to obtain a valid approximate mapping from electromyography (EMG) signals to angular position and velocity of a joint of interest. Though ANNs have been explored previously [3], this work focuses on the accurate mapping of both angular trajectory and velocity with one EMG signal rather than multiple.

Once angular trajectories are provided from this model, there are multiple applications that can take advantage of it, such as active orthotic devices. Many diseases and injuries can impair joint mobility compared with normal reference values [4]. Therefore, the design of such device should consider trajectory restraints. Furthermore, volitional behavior during rehabilitation contributes to treatment effectiveness with respect to passive roles [5]. In order to address this factor, a trajectory compensator was added only when the individual could not exert enough force to achieve the desired angle.

Based on the aforementioned, a validated neuromusculoskeletal model to obtain the angular position and velocity of a determinate articulation using raw EMG signals is proposed here. The model is based on a differential neural network identifier, and the learning laws for the parameter estimation are based on Lyapunov theory ensuring the ultimate boundedness of the error between the estimated parameters and the actual approximation parameters. The data collection, training, validation, and test implementation for the DNN musculoskeletal model are described. In addition, the design of the controller ensures the fulfillment of predefined restrictions. The restrictions limit the orthosis trajectories in a fixed angular range.

II. Problem Statement

A valid model to map the raw EMG signal to the angular position of a particular joint is needed. This can be expressed as the estimation of the unknown dynamics $h_i : \mathbb{R}^2 \times \mathbb{R}$ for $\dot{z}_i(t) = h_i(z_i(t), u_i(t))$, where the state vector $z_i \in \mathbb{R}^2$ represents the angle position and angular velocity of the i-th joint, and $u_i(t)$ is the raw EMG signal from the agonist muscle. To solve this stage, a non-parametric identifier can be used, in this way the state $y_i \in \mathbb{R}^2$ represents the angular position and velocity mapped from the raw EMG signal of the i-th agonist muscle. Such identifier ensures the convergence to the origin or at least to a zone near the origin of the identification error $\Delta_i = y_i - z_i$.

In the second stage, we obtain the virtualization of the active orthosis device. This is solved using the CAD model of the real orthosis. The dynamics to obtain the position for all the degrees of freedom (DoF) q and the velocity $\dot{q}$ from an input torque τ can be used for the numerical tests. For the upper-limb orthosis, five DoF were considered, thus, the sub-index i represents each decentralized subsystem for the i-th available movement of the device $i = \{\overline{1,5}\}$.

Considering the path generator from the neuromusculoskeletal model given by the trained identifier, the following issue resides in the design of a hybrid trajectory $x_i^* : \mathbb{R}^+ \to \mathbb{R}^2$, such that the descentralized states of the virtual orthosis $x_i = [q_i,\ \dot{q}_i]^\top$ reach a set constant point $x_i^+ \in \mathbb{R}$, taking into account the path given by z_i. To achieve this, the following set of desired reference trajectories has been proposed

$$x_i^*(t) = \begin{cases} y_i(t) & \text{if} \quad A_i, \\ y_i(t) + z_{i,s}(t) & \text{if} \quad B_i, \end{cases} \tag{1}$$

where $A_i = |y_{2,i}| \geq \alpha_i$ or $t \leq t_B$, $B_i = |y_{2,i}| < \alpha_i$ and $|x_i^+ - y_{1,i}| \geq \beta_i$ and $t > t_B$, with $\alpha_i \in \mathbb{R}_+$, $\beta_i \in \mathbb{R}^+$,

A. Lozano is with the Unidad Profesional Interdisciplinaria de Biotecnología - Instituto Politécnico Nacional, 07340 Mexico City, Mexico.

D. Cruz-Ortiz is with the Unidad Profesional Interdisciplinaria de Biotecnología - Instituto Politécnico Nacional, Mexico City, Mexico.

M. Ballesteros and I. Chairez are with the Unidad Profesional Interdisciplinaria de Biotecnología - Instituto Politécnico Nacional, Mexico City; and with the Tecnologico de Monterrey, School of Engineering and Sciences.

978-1-7281-1178-0/21/$31.00 ©2021 IEEE

$t_B \in \mathbb{R}_+$, $t_B > t_0$ and $z_{i,s}\colon \mathbb{R}^+ \to \mathbb{R}^2$ is a function with sigmoidal signals to complete the path.

The last step requires the design of the control algorithm to solve the trajectory tracking for the virtual orthosis. The aim of the controller is to drive the states of the orthosis $x_i = [q_i,\ \dot{q}_i]^\top$ to the desired reference $x_i^* \in \mathbb{R}^2$, such that,

$$\lim_{t\to\infty} \|e_i\|^2 \leq \eta_i, \quad \eta_i \in \mathbb{R}^+, \tag{2}$$

where $e_i = x_i - x_i^*$ defines the tracking error of the virtual orthosis device (VOD) but subject to the following set of position constraints $\|q_i - x_i^+\| > \psi_i, \quad \forall x_i^+ \in \partial\Theta_i$ where $\psi_i \in \mathbb{R}^+\backslash\{0\}$ defines a safety factor to avoid the transgression of the position constraints and $\partial\Theta_i$ describes the boundary of the working space in the i-th joint of the VOD that should be established according to the anthropometric ranges.

III. ANN NEUROMUSCULOSKELETAL MODEL

Based on the models described in the literature to represent the neuromusculoskeletal systems [6, 7], the following ODE in a general form represents such dynamics.

$$\begin{gathered}\dot{z}_i(t) = h_i(z_i(t), u_i(t)) = f_i(z(t)) + g_i(z_i(t))u_i(t),\\ z_i(0) = z_{0,i},\end{gathered} \tag{3}$$

where $z_i \in \mathbb{R}^2$, $z_i = [\theta_i, \dot{\theta}_i]^\top$, θ_i is the angular joint position, $\dot{\theta}_i$ is the angular velocity, $u_i \in \mathbb{R}$ is the raw EMG signal, $f_i\colon \mathbb{R}^2 \to \mathbb{R}^2$ is a nonlinear continuous function, $g_i\colon \mathbb{R}^2 \to \mathbb{R}^2$ is a nonlinear continuous function associated with the input, and $z_{0,i}$ are the initial conditions. Notice that this model represents the contribution of a single raw EMG signal, however more signals can be included. Considering the nature of the system and the input-output signals, the input raw EMG signal and the output signal, position and velocity of a determinate articulation are bounded such that

$$u_i^2(t) \leq u_i^+ < +\infty, \quad \|z_i\|^2 \leq z_i^+ < +\infty, \quad \forall t \in \mathbb{R}^+, \tag{4}$$

we use the model to represent the contribution of the EMG signal obtained from the Biceps Brachii to regulate elbow flexion and extension.

A. Neural Network Representation

For (3), taking into account the approximation properties of ANNs [8–11], the ANN representation is

$$\begin{gathered}\dot{z}_i(t) = A_i z_i(t) + \phi_{1,i}\psi_{1,i}(z_i(t))\\ +\phi_{2,i}\psi_{2,i}(z_i(t)) + \nu_i(z_i(t)),\end{gathered} \tag{5}$$

where $A_i \in \mathbb{R}^{2\times 2}$ is a Hurwitz matrix, $\phi_{1,i} \in \mathbb{R}^{2\times p}$ and $\phi_{2,i} \in \mathbb{R}^{2\times q}$ are the weights of the ANN structure, $\psi_{1,i}\colon \mathbb{R}^2 \to \mathbb{R}^p$ and $\psi_{2,i}\colon \mathbb{R}^2 \to \mathbb{R}^q$ are vectors with the activation functions and $\nu_i\colon \mathbb{R}^2 \to \mathbb{R}^2$ represents the approximation error which is bounded based on the approximation theorem based on the sigmoid functions superposition [9], i.e,

$$\|\nu_i\|^2 \leq \nu_{0,i}^+ + \nu_{1,i}^+ u_i^+, \quad \forall t \in \mathbb{R}^+, \tag{6}$$

where $\nu_{0,i}^+$ and $\nu_{1,i}^+$ are positive constants. Sigmoids are the class of activation functions for this ANN representation, each element in $\psi_{1,i}$ and $\psi_{2,i}$ obeys the following function,

$$(\psi_{j,i})_k(z) = \left(1 + e^{-\left(b_{ijk}^\top z + c_{ijk}\right)}\right)^{-1}, \tag{7}$$

where $b_{ijk} \in \mathbb{R}^2$ and $c_{ijk} \in \mathbb{R}$ are the sigmoid free-parameters for the k-th element of the j-th array in the approximation for the i-th articulation, $i = \{\overline{1,5}\}$, $j = \{\overline{1,2}\}$ and $k = \{\overline{1,p}\}$ when $j = 1$ and $k = \{\overline{1,q}\}$ when $j = 2$.

The following assumptions are considered for the design of the DNN identifier.

Assumption 1. *Based on the form of the activation functions* (7)*, which satisfy the sector condition [12], the following inequalities hold,* $\|\psi_{j,i}(z_a)\|_{Z_{j,i}}^2 \leq \|z_a\|_{C_{j,i}}^2$, $\|\psi_{j,i}(z_a) - \psi_{j,i}(z_b)\|_{\Lambda_{j,i}}^2 \leq \|z_a - z_b\|_{D_{j,i}}^2$.

Assumption 2. *The weights fitting the approximation are unknown but are bounded in the following sense.* $\phi_{j,i}\Lambda_{\phi_{j,i}}\phi_{j,i}^\top \leq \Phi_{j,i}$*, where* $\Phi_{j,i} = \Phi_{j,i}^\top \in \mathbb{R}^{2\times 2}$ *and* $\Lambda_{\phi_{j,i}}$ *are positive definite matrix of proper dimensions.*

B. Differential Neural Network Identifier

The proposed identifier consists of a classical DNN as the described in [12], Chapter 2.

$$\begin{gathered}\dot{y}_i(t) = A_i y_i(t) + \underline{\phi}_{1,i}(t)\psi_{1,i}(y_i(t)) + \underline{\phi}_{2,i}(t)\psi_{2,i}(y_i(t)),\\ \dot{\underline{\phi}}_{1,i}(t) = -K_{1,i}P_i\Delta_i\psi_{1,i}^\top(y_i(t)),\\ \dot{\underline{\phi}}_{2,i}(t) = -K_{2,i}P_i\Delta_i\psi_{2,i}^\top(y_i(t))u_i(t),\end{gathered} \tag{8}$$

where $y_i \in \mathbb{R}^2$ represents the state of the identifier, $\underline{\phi}_{1,i}\colon \mathbb{R}_+ \to \mathbb{R}^{2\times p}$ and $\underline{\phi}_{2,i}\colon \mathbb{R}_+ \to \mathbb{R}^{2\times q}$ are the adaptive weights, $\Delta_i = y_i - z_i$ is the identification error, and $K_{1,i} \in \mathbb{R}^{2\times 2}$, $K_{2,i} \in \mathbb{R}^{2\times 2}$ and $P_i \in \mathbb{R}^{2\times 2}$ are positive definite matrices.

Theorem 1. *[12] Consider the uncertain system* (3) *represented by* (5)*, and considering* (4)*,* (6)*, Assumption 1 and Assumption 2. If the identifier with adaptive weights* (8) *has* $K_{1,i} \in \mathbb{R}^{2\times 2}$ *and* $K_{2,i} \in \mathbb{R}^{2\times 2}$ *positive definite and* P_i *is the solution of the following matrix Riccati equation [13],* $P_iA_i + A_i^\top P_i + P_iR_iP_i + Q_i = 0$ *where* $Q_i = Q_{0,i} + D_{1,i} + D_{2,i}u_i^+$, $R_i = \Phi_{1,i} + \Phi_{1,2} + 2\Upsilon_i I_2$, $\Upsilon_i \in \mathbb{R}^+\backslash\{0\}$ *and* $Q_{0,i} = Q_{0,i}^\top \in \mathbb{R}^{2\times 2}$ *is a positive definite matrix. Then, the weights dynamics are bounded and the identification process is asymptotically consistent.*

C. Training and Validation of the proposed DNN Identifier

For this study, the model represents the system mapping the raw EMG signal, measured from the Biceps Brachii muscle to the angular position in the flexion and extension movement of the elbow. In general, other muscles and articulations follow the same procedure, however here we restrict the identification for the elbow.

1) Data collection: A three-dimensional (3D) printed analog goniometer was used to obtain the angular trajectory, the angle/voltage relationship was trained with an $\ell_1 + \ell_2$ regression, while a single MyoWare™ sensor positioned on the Biceps brachii muscle operating at 3.3 Volts was used to obtain the EMG signals. Both sensors were connected to an Arduino Uno® clocked at 9600 bauds, and interfaced with

Python via UART. The data was then cut into equal segments (without any additional preprocessing steps) and stored in a comma-separated value file to be later exported to Matlab-Simulink® and used to train the DNN.

To obtain homogeneous signals, the following protocol was proposed: Initiate at a standing position with the arm fully extended, forming a 180 degree angle between the humerus and the radius (0s to 15s), begin first flexion (15s to 25s), rest (25s to 40s), execute first extension, return to initial condition (40s to 50s), rest (50s to 65s), begin second flexion (65s to 75s), rest (75s to 90s), begin second extension, returning to initial condition (90s to 100s), rest (100s to 115s).

Notice that the proposed 3D printed goniometer provides only the angular position (θ_i) of the i-th upper-limb articulation. Nevertheless, this device does not provide the angular velocity ($\dot{\theta}_i$) since does not includes velocity sensors in its electronic instrumentation, as a consequence the angular velocity is not available online. Therefore, to obtain the complete state z_i it is necessary to implement an algorithm to estimate angular velocity. The velocity estimation problem has been solved by using the so-called state observers. However, most of them offered only asymptotic convergence that does not match with the DNN training requirements. Therefore, the estimation of $\dot{\theta}_i$ requires the application of a finite-time observer. One of the most remarkable observer based on the sliding-mode theory is the Super Twisting algorithm (STA), that can be used like state estimator and robust differentiator [14, 15]. In this paper, the STA is proposed as robust differentiator considering the following description. Let $\upsilon_{1i} = \theta_i$ where $\theta_i \in \mathbb{R}$ is the signal to be differentiated and defining $\upsilon_{2i}(t) = \dot{\theta}_i(t)$, taking into account that $|\ddot{\theta}_i| \leq \theta_i^+$, it is possible to obtain the following auxiliary equation $\dot{\upsilon}_{1i}(t) = \upsilon_{2i}(t)$, $\dot{\upsilon}_{2i}(t) = \ddot{\theta}_i(t)$. The STA to obtain the derivative of θ_i takes the following form,

$$\frac{d\hat{\upsilon}_{1i}(t)}{dt} = \hat{\upsilon}_{2i}(t) - \mu_{1i}|\Delta_{\upsilon i}(t)|^{0.5}\text{sign}(\Delta_{\upsilon i}(t)),$$
$$\frac{d\hat{\upsilon}_{2i}(t)}{dt} = -\mu_{2i}\text{sign}(\Delta_{\upsilon i}(t)),$$

where $\mu_{1i} \in \mathbb{R}^+\backslash\{0\}$ and $\mu_{2i} \in \mathbb{R}^+\backslash\{0\}$ are the STA gains, the observation error is defined by $\Delta_{\upsilon i}(t) = \hat{\upsilon}_{1i}(t) - \upsilon_{1i}(t)$. The output of the differentiator is given by $\dfrac{d\hat{\upsilon}_{1i}(t)}{dt}$ with $i = \{\overline{1,5}\}$ describing the i-th upper-limb articulation [15].

2) Training Stage: The proposed model based on a DNN identifier has adaptive laws to obtain the estimation of the unknown parameters (8). However, other free parameters in this DNN structure can be tuned to obtain better results, here we used an additional stage denoted as training, using an early stopping like algorithm to modify the initial parameters, the criterion used is the integral of the identification error norm.

IV. Virtual Model of the Orthosis Device

The orthosis device considered in this work is a modification of the device presented by Merchant et al. [16]. Here, it should be noticed that the considered device was integrated by four main segments that are: hand, forearm, shoulder, and shoulder pad (see Figure 1) each of them designed taking into account the anthropometric dimensions presented in [16]. Figure 1 provides an isometric view of the orthosis model obtained from a computer-assisted (CAD) draw design made with the software Solidworks. The orthotic device is integrated by five DoF denoted by q_i with $i = \{\overline{1,5}\}$, all of them distributed around the three main anatomical upper-limb joints, that is, two DoF in the Scapulohumeral articulation (q_5 and q_4), one in the elbow articulation (q_3) and two Radiocarpal articulation (q_2 and q_1). To obtain the virtual model used in this manuscript, the orthotic CAD model from SolidWorks® was exported to an XML file. Then, using the Simscape toolbox was imported to the Matlab-Simulink® environment. The use of the Simscape® toolbox gives a virtual model of the orthotic system in which it is possible to implement different identification algorithms and control schemes in the Matlab-Simulink® environment.

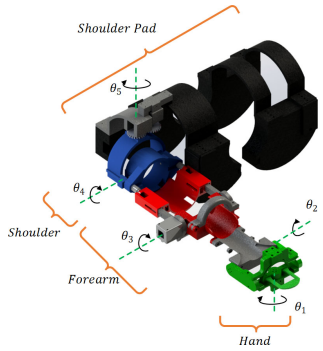

Fig. 1. Segments of upper-limb VOD.

V. Electromyographic Control Algorithm

Introduce the following second order differential equation that represents in a general form the VOD dynamic model.

$$\ddot{q}(t) = F(q(t), \dot{q}(t)) + \Gamma(q(t))\tau(t) + \chi(q(t), \dot{q}(t)), \quad (9)$$

where $q \in \mathbb{R}^5$, $\dot{q} \in \mathbb{R}^5$ and $\ddot{q} \in \mathbb{R}^5$ represent the vectors of joint positions, velocities and accelerations of the upper-limb orthosis device, respectively. The drift term $F : \mathbb{R}^5 \times \mathbb{R}^5 \to \mathbb{R}^5$ gathers all the terms associated with gravitational effects and the components of Coriolis matrix for the orthosis device. The following assumption is assumed to be valid for the drift term.

Assumption 3. *The drift term F is uncertain but satisfies the following upper bound $\|F(q(t), \dot{q}(t))\|^2 \leq f_0 + f_1\|x(t)\|^2$, where $f_0 \in \mathbb{R}^+\backslash\{0\}$ and $f_1 \in \mathbb{R}^+\backslash\{0\}$ and $x \in \mathbb{R}^5$ is the vector defined such that $x = \begin{bmatrix} q & \dot{q} \end{bmatrix}^\top$.*

In (9), the matrix $\Gamma : \mathbb{R}^5\times \to \mathbb{R}^{5\times 5}$ represents the state depended matrix that characterizes the control input defined by $\tau \in \mathbb{R}^5$. This work assumes that Γ is bounded satisfying

Assumption 4. *The matrix Γ is unknown but bounded by two positive constants γ^- and γ^+ such that $0 < \gamma^- \leq \|\Gamma(q)\| \leq \gamma^+ < \infty \ \ \forall q \in \mathbb{R}^5$.*

The nonlinear function $\chi : \mathbb{R}^5 \times \mathbb{R}^5 \rightarrow \mathbb{R}^5$ in (9), represents the internal uncertainties and external perturbations acting over the orthotic device. Here, the function χ satisfies

Assumption 5. *The nonlinear function is unknown but admits the following upper bound,* $\|\chi(q,\dot{q})\|^2 \leq \chi_0^+ + \chi_1^+\|x(t)\|^2$, *with* χ_0^+ *and* χ_2^+ *being positive constants.*

A. State variables representation and system decomposition

Consider the dynamic model given in (9) that describes a fully actuated upper-limb orthosis device with five DoF. By using the state variables theory and defining the state variables $x_{1,i} = q_i$ and $x_{2,i} = \dot{q}_i$ with $i = \{\overline{1,5}\}$ the system given in (9) can be represented as a system decomposition described by a set of five second order subsystems satisfying the following equation [17, 18].

$$\begin{aligned} \dot{x}_{1,i} &= x_{1,i}, \\ \dot{x}_{2,i} &= F_i(x_i(t)) + \Gamma_i(x_{1,i}(t))\tau(t) + \chi_i(x_i(t)) + \sum_{j=1}^{5} \Gamma_{i,j}\tau_j. \end{aligned} \tag{10}$$

where $x_{1,i}$ and $x_{2,i}$ describe the $i-$th states of the system.

B. Sliding mode control for the virtual orthosis device

The trajectory tracking control between the states of the VOD and the set of the desire references trajectory can be solved by several control schemes. Nevertheless, most of the classics control schemes does not consider the fulfillment of position constraints.

Here, it should be noticed that in the rehabilitation field the consideration of the angular constraints can provide several advantages in the rehabilitation process of the patient, being one of the most relevant to avoid possible injury due to the overshot effect in the orthotic rehabilitation system.

To this end, the current work proposes a state feedback controller based on the sliding mode theory that considers in its structure the inclusion of some mathematical terms to ensure the fulfillment of the position constraints in the VOD. Taking into account the system decomposition given in (10) and considering the tracking error of each joint that integrates the VOD defined in (2) with e_i defined such that $e_i = \begin{bmatrix} e_{1,i} & e_{2,i} \end{bmatrix}^\top$. The first step to define the control law is to introduce the sliding surface σ_i given by $\sigma_i(t) = e_{2,i}(t)\gamma_i + e_{1,i}(t)$ where γ_i is a positive constant. To satisfy the control problem presented in (2) the following control structure has been proposed.

$$\tau_i(t) = -k_i(t)\text{sign}(\sigma_i(t)), \tag{11}$$

where the control gain k_i satisfies the following structure

$$k_i(t) = \Gamma_i^{-1}(x_{1,i})\gamma_i^{-1}\left(\frac{r_i}{\iota_i(t)} + \rho_i\right), \tag{12}$$

with r_i being a positive constant that regulates the convergence velocity of each joint of the virtual device. The time varying function ι_i has the role of an adaptive gain increasing the control gain each time that the trajectories of the orthotic device approach the predefined constraints. The adaptive gain ι_i satisfy the following structure

$$\iota_i(t) = \frac{\inf_{x_i^+ \in \partial\Theta_i}\{d(q_i, x_i^+)\}^2}{\inf_{x_i^+ \in \partial\Theta_i}\{d(q_i, x_i^+)\}^2 + \epsilon},$$

with $\epsilon \in \mathbb{R}^+\backslash\{0\}$ being a small positive constant and the function $\inf_{x_i^+ \in \partial\Theta_i}\{d(q_i, x_i^+)\}^2$ describing the smallest distance between the set of predefined position constraints and the trajectory performed by the VOD in the i-th joint. In (12), the parameter ρ_i represents a nonlinear compensation satisfying $\rho_i = |\gamma_i^{-1}|(\sqrt{f_{0,i}} + \sqrt{f_{1,i}}\|e_i\|) + |e_{2,i}|$.

Theorem 2. *Consider the system decomposition given in* (10) *subject to the constraints in closed-loop with the control law* (11). *If there exist a positive constant* γ_i *such that the gain* ρ_i *is positive, and a small positive constant* ϵ *such that* $0 < \iota_i < 1$. *Then the positiveness of the control gain* k_i *is guaranteed and as a consequence the tracking error reaches the sliding surface* $\sigma_i(t) = 0$ *in a finite time* T_i^* *defined by* $T_i^* = |\sigma_i|\left(2\min_{t\in\mathbb{R}^+}\left\{\frac{r_i}{\iota_i(t)}\right\}\right)^{-0.5}$.

Proof. The proof is omitted due to the limited space, a similar approach can be consulted in [19]. □

To summarize the control algorithm implementation over the VOD, Figure 2 shows a detail implementation diagram to verify the interaction between all sections previously described. In this figure it is clear how the DNN identifier interacts with the proposed control algorithm to ensure the VOD closed-loop system.

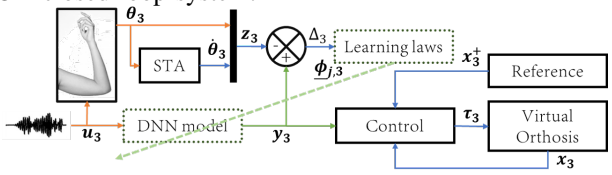

Fig. 2. Control diagram of VOD.

VI. Numerical Simulations

The proposed DNN structure (8) considered four neurons for each $\psi_{i,j}$ array, thus $p = q = 4$. The initial condition for the states of the DNN were fixed as $y_3(t_0) = [0,\ 0]^\top$. Table I shows the change in the identification error with respect to the number of epochs. Figure 3 shows the identification

TABLE I
Integral of the identification error in the DNN training stage.

Epochs	1	4	6	8	10
$\int_{t_0}^{t_f} \lvert\Delta_i\rvert dt$	109.02	108.43	108.32	108.28	108.27

results once the initial conditions and free-parameters were fixed after the training stage. The first graph (a) shows the EMG input signal, the second and third subfigures (b and c) depict the comparison between the actual data and the DNN states, position and velocity respectively.

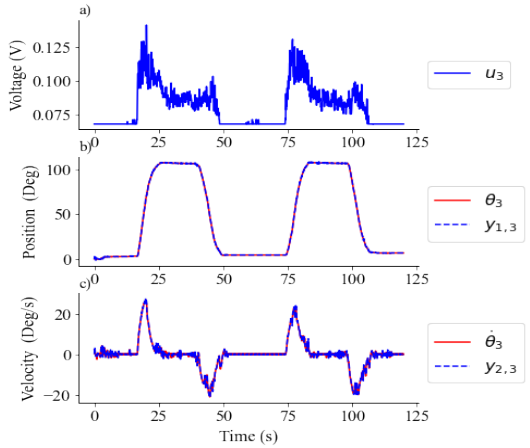

Fig. 3. (a) EMG signal used to train DNN (b) DNN angular trajectory prediction after testing vs real angular trajectory (c) DNN angular velocity prediction after testing vs real angular velocity.

In Figure 4, the results after the implementation of the control strategy using the Sliding Mode control with restrictions and the path generator given by the DNN model and the modify trajectory (1) are depicted. The function $z_{3,s}(t)$ consists in the addition of two sigmoid functions one positive and one negative, considering the final point given by the steady trajectory y_3 and the fixed point $x_3^+ \approx 100$.

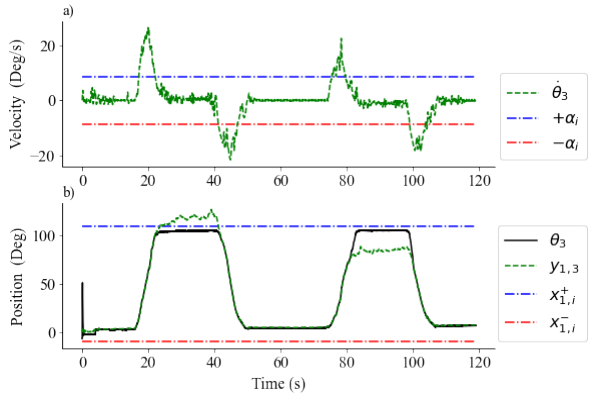

Fig. 4. (a) Angular velocity predicted by DNN. (b) Angular trajectory predicted by DNN, complemented by barrier restrictions and hybrid trajectory.

VII. Conclusion

In this work, a neuromusculoskeletal model based on DNNs was presented. The model served as a path generator using raw EMG signals from the Biceps Brachii muscle to regulate a virtual model of an active orthotic device for the upper limb. The validated model was the outcome of the adaptive adjustment parameters or weights and additional training (Algorithm 1) of the proposed DNN identifier. The ANN model, along with the proposed control scheme, ensured that the user reaches a fixed point in the angular range without getting out of the natural path given by the muscle signals in the transient stages.

References

[1] Yasuharu Koike and Mitsuo Kawato. Estimation of dynamic joint torques and trajectory formation from surface electromyography signals using a neural network model. *Biological cybernetics*, 73(4):291–300, 1995.

[2] James WL Pau, Shane SQ Xie, and Andrew J Pullan. Neuromuscular interfacing: Establishing an EMG-driven model for the human elbow joint. *IEEE Transactions on biomedical engineering*, 59(9):2586–2593, 2012.

[3] Suncheol Kwon and Jung Kim. Real-time upper limb motion estimation from surface electromyography and joint angular velocities using an artificial neural network for human–machine cooperation. *IEEE transactions on Information Technology in Biomedicine*, 15(4):522–530, 2011.

[4] JM Soucie, C Wang, A Forsyth, S Funk, M Denny, KE Roach, D Boone, and Hemophilia Treatment Center Network. Range of motion measurements: reference values and a database for comparison studies. *Haemophilia*, 17(3):500–507, 2011.

[5] John Whyte, Marcel P Dijkers, Tessa Hart, Jarrad H Van Stan, Andrew Packel, Lyn S Turkstra, Jeanne M Zanca, Christine Chen, and Mary Ferraro. The importance of voluntary behavior in rehabilitation treatment and outcomes. *Archives of physical medicine and rehabilitation*, 100(1):156–163, 2019.

[6] Thomas S Buchanan, David G Lloyd, Kurt Manal, and Thor F Besier. Neuromusculoskeletal modeling: estimation of muscle forces and joint moments and movements from measurements of neural command. *Journal of applied biomechanics*, 20(4): 367–395, 2004.

[7] J. W. L. Pau, S. S. Q. Xie, and A. J. Pullan. Neuromuscular Interfacing: Establishing an EMG-Driven Model for the Human Elbow Joint. *IEEE Transactions on Biomedical Engineering*, 59(9):2586–2593, 2012.

[8] N. E. Cotter. The Stone-Weierstrass theorem and its application to neural networks. *IEEE Transactions on Neural Network*, 1:290–295, 1990.

[9] George Cybenko. Approximation by Superpositions of a Sigmoidal Function. *Mathematics of control, signals and systems*, 2(4):303–314, 1989.

[10] Silvia Ferrari and Robert F. Stengel. Smooth function approximation using neural networks. *IEEE Transactions on Neural Networks*, 16(1):24–38, 2005.

[11] Namig J. Guliyev and Vugar E. Ismailov. On the approximation by single hidden layer feedforward neural networks with fixed weights. *Neural Networks*, 98:296–304, 2018.

[12] Alexander S. Poznyak, Edgar N. Sanchez, and Wen Yu. *Differential Neural Networks for Robust Nonlinear Control*. World Scientific Publishing, 2001.

[13] A. Poznyak. *Advanced Mathematical Tools for Automatic Control Engineers: Volume 1: Deterministic Systems*, volume 1. Elsevier Science, 2008.

[14] Jorge Davila, Leonid Fridman, and Arie Levant. Second-order sliding-mode observer for mechanical systems. *IEEE Transactions on Automatic Control*, 50(11):1785–1789, 2005.

[15] Arie Levant. Robust exact differentiation via sliding mode technique. *automatica*, 34(3):379–384, 1998.

[16] Roberto Merchant, David Cruz-Ortiz, Mariana Ballesteros-Escamilla, and Isaac Chairez. Integrated wearable and self-carrying active upper limb orthosis. *Proceedings of the Institution of Mechanical Engineers, Part H: Journal of Engineering in Medicine*, 232(2):172–184, 2018.

[17] Ivan Salgado, Isaac Chairez, Oscar Camacho, and Cornelio Yañez. Super-twisting sliding mode differentiation for improving pd controllers performance of second order systems. *ISA transactions*, 53(4):1096–1106, 2014.

[18] David Cruz-Ortiz, Isaac Chairez, Vadim I Utkin, and Alexander Poznyak. Decentralized sliding-mode control of robotic manipulator with constraint workspace: a finite-convergent barrier lyapunov approach. In *2019 16th International Conference on Electrical Engineering, Computing Science and Automatic Control (CCE)*, pages 1–6. IEEE, 2019.

[19] D Cruz-Ortiz, I Chairez, and A Poznyak. Adaptive sliding-mode control with integral compensation for robotic devices with state constraints. *IFAC-PapersOnLine*, 51(22):506–511, 2018.